JOURNAL OF ENGINEERED FIBERS AND FABRICS

Original research article

Journal of Engineered Fibers and Fabrics
Volume 21: 1–12

DOI: 10.1177/15589250261440928
journals.sagepub.com/home/jef
Sage

Evaluating geometric accuracy of embroidered QR codes for smart tag applications

Breitmozere Inga[1] and **Domskiene Jurgita**[1]

Abstract

Embroidery offers a durable and attractive option for textile smart tags, but the effect of embroidery parameters on QR code accuracy and readability is still mostly unexamined, even in earlier studies. This study aims to evaluate the feasibility of using embroidery for functional QR code integration on woven and knitted fabrics by assessing the geometric accuracy of the Finder Pattern element, as defined by ISO/IEC 18004:2024. The analysis focusses on how module size, fabric type, stitch type and scan line direction affect dimensional stability. The experimental results showed that the deviations in the modules were systematic in all analysed variables. The most accurate geometry was achieved with an 8.8 mm Finder Pattern size, yielding negligible deviation (≈0%). Woven fabric and vertical scan line direction of knitted fabric demonstrated minimal distortions (–2% to +2.6%), whereas horizontal scan line direction for knitted fabric showed up to four times greater deviations (–8.8%). Stitch type influenced accuracy differently: satin stitch ensured precise shaping of individual modules, while tatami stitch preserved the overall Finder Pattern size. Statistical ANOVA analysis confirmed the most significant variables, with size being the dominant factor affecting total Finder Pattern length deviation. The research demonstrated that the Finder Pattern assessment method based on ISO/IEC 18004:2024 could be used to predict the quality of an embroidered QR code. The results prove that embroidery can support functional QR code production when parameters are carefully optimised. Future research should address durability under wear and washing conditions and expand quality assessment beyond the Finder Pattern.

Keywords

embroidery, QR, Finder Pattern, image analysis, module deviation, distortion

Received: 30 November 2025; accepted: 25 March 2026

Introduction

Barcodes are optically machine-readable representations of data that encode information. The Universal Product Code (UPC) is a well-known example of barcodes employed in a one-dimensional (1D) format, characterised by variations in the widths and spacings of parallel lines, commonly known as linear barcodes. Advances in data encoding have led to the development of two-dimensional (2D) barcodes, including Quick Response (QR) codes, which utilise geometric patterns, such as dots, rectangles, or rounded shapes, to store more complex data. Initially dependent on dedicated optical scanners, barcode technology has evolved to support decoding by image-based devices, such as

[1]Faculty of Mechanical Engineering and Design, Kaunas University of Technology, Lithuania

Corresponding author:
Breitmozere Inga, Faculty of Mechanical Engineering and Design, Kaunas University of Technology, Studentu str. 56, Kaunas, LT 51424, Lithuania.
Email: inga.breitmozere@ktu.edu

smartphones, and is now universally accessible. QR codes fulfil several functions, such as capturing information, redirecting users to websites, advertising, preventing counterfeiting, and facilitating mobile payments. Integrated with big data analytics, they enable advanced applications, including garment customisation and personalised design.[1]

QR and similar technologies, such as Radio Frequency Identification (RFID), and Near-Field Communication (NFC) have attracted the attention of different stakeholders as a result of the European Commission's initiative to introduce Digital Product Passport (DPP). DPP is a digital document that provides key information about a product (origin, composition, reuse, repair, disposal, etc.) and secures transparency, sustainability, and digitalisation development,[2–4] consistent with trends reported in global markets.[5] Ordinarily, the requirements of DPP can be met by smart tags, which are increasingly being integrated into products across various industries to improve traceability and transparency. Each technology offers unique benefits, as described in the following examples.[6] Compared to NFC and RFID, QR codes are more cost-effective, easier to integrate, and more durable.[7,8] These advantages make QR codes the preferred choice in the market. In addition, combinations of multiple technologies are currently being developed, demonstrating the potential of QR technology in the development of innovative tags. For example, a single tag may incorporate both QR codes and RFID to leverage the advantages of each.[9] Smart tags are designed by integrating functional inks into QR codes, enabling them to respond to environmental conditions, such as temperature.[10] Photochromic ink has been incorporated into the design of QR codes to enable changes to the data matrix (e.g. URL addresses) under specific light conditions.[6] Recent research has shown that the use of multiple colour-based QR images can significantly enhance the data capacity of a particular QR code.[11]

The mandatory adoption of Digital Product Passports (DPP) for textiles sold in Europe by 2030[12] is increasing the demand for durable and traceable labelling solutions within the fashion industry. Among textile-based smart tag technologies, QR codes have emerged as the most widely used, extensively analysed, and continuously improved through various integration techniques. Fan et al.[13] developed a smart photochromic fabric capable of storing image-based information patterns, Li et al.[14] introduced a method for displaying coloured QR codes on fabric using thermochromic fibres. A few projects have also proposed the integration of QR codes into textile designs.[15,16]

To link technological possibilities with practical textile applications, embroidery may be considered a viable approach. Traditional embroidery techniques are widely employed for producing high-quality, durable images on textiles, and attempts have been made to apply this method to replicate QR codes on textile surfaces.[17,18] Machine embroidery can be applied to nearly any fabric regardless of its structure or composition. However, if threads and embroidery parameters are inappropriately selected in relation to pattern details, visual quality issues may arise. During the embroidery stitching process, local deformations of the fabric may occur depending on the placement pattern of introduced threads.[19,20] Designing embroidery patterns requires careful consideration of the anisotropic appearance of stitched threads, stitching density and their directional alignment,[20,21] as well as the choice of supporting non-woven interlining[19,22,23] and other parameters, all of which are critical for effectively conveying pattern transfer and details through embroidery. Parameters must be chosen carefully, especially when embroidering knitted materials, as geometry and details of embroidered pattern depend on the structure of knitted fabric.[19] Embroidery has emerged as a promising technique for the development of smart tags, particularly RFID antennas.[24,25] Studies have investigated the impact of embroidery parameters such as stitch direction and stitch density on antenna performance.[26] In machine embroidery, it is crucial to assess not only common defects, such as yarn floating, missing stitches, joint defects, and misregistration,[27] but also potential contour distortions and geometric inaccuracies, especially near edges and corners[28,29] These defects can influence not only the quality and aesthetics of the final pattern but also impair the functionality of smart tags and other e-textile elements.[24,25,30]

Although previous research has explored embroidery techniques as promising design method for textile-based smart tag development, this approach appears particularly suitable for creating reliable and durable tags incorporating QR codes. However, only few scientific studies have addressed this topic, and most have focussed primarily on the application of embroidered QR codes rather than their quality. The effect of embroidery parameters on the geometric accuracy of QR codes, and consequently on their readability, remains largely unexplored.

This study aims to assess the geometric accuracy of embroidered QR code and evaluate the feasibility of using embroidery for functional QR codes development on woven and knitted fabric. Standard ISO/IEC 18004:2024[31] was adapted to define the quality of QR code based on embroidered Finder Pattern element assessment. The research investigates the influence of the module size, fabric type, stitch type, and scan line direction on the dimensional deviations of Finder Pattern element, which are critical for QR code readability.

Sample preparation

For this study, a version 2 QR code was generated using the free online tool 'TQRCG'.[32] This is a classic QR code, which consists of black and white square modules of a fixed size, arranged in a specific pattern across designated areas such as separators, timing patterns, Finder Patterns, alignment patterns, and the content region (Figure 1). Each pattern in the QR code serves a specific function.[31,33,34]

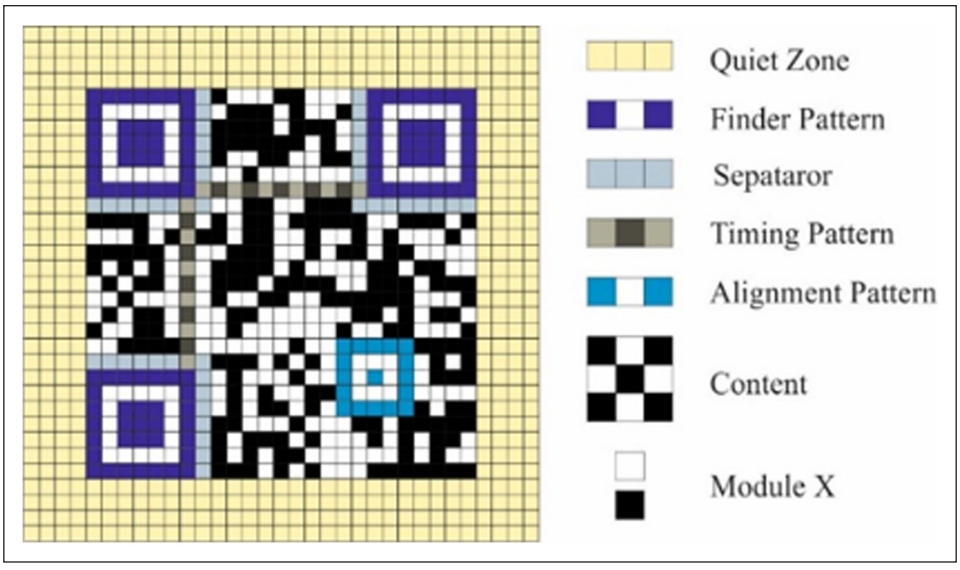

Figure 1. Structure of the Generated QR Code.

Table 1. Dimensions of Finder Pattern and corresponding modules.

No.	Finder Pattern size AB_T, mm	Single module size X_T, mm	Triple module size $3X_T$, mm
1	15.00	2.14	6.43
2	12.00	1.71	5.14
3	10.00	1.43	4.29
4	7.00	1.00	3.00

Scanning algorithms for QR code first detect the Finder Pattern, which defines the symbol position, orientation, and scale, enabling recognition of the QR code among other graphical elements. Successful Finder Pattern detection enables reconstruction of the QR code grid and identification of other functional elements, whereas distortions in the Finder Pattern may prevent recognition and render the QR code unreadable.[35,36]

Finder Pattern elements were extracted from the generated QR code as separate units for embroidery and later analysis. The size of the Finder Pattern directly depends on the overall dimensions of the QR code, as its structure is defined by the ISO/IEC 18004 standard.[31] The sizes were chosen in accordance with findings from previous studies[15,37] and with consideration of the technical limitations of the embroidery technique.[21] Table 1 presents the dimensions of Finder Pattern element, along with the theoretical module X_T (where X represents the module dimension in millimetres) values for single (X_T) and triple ($3X_T$) modules.

Finder Pattern elements are located in the three corners of the QR code and are scanned through their centres along both the vertical and horizontal axes (Figure 2(a)) and recognised along scan line AB (Figure 2(b)). Each pattern consists of three components: 3×3 square of black modules (C), 5×5 square of white modules (D), and 7×7 square of black modules (E; Figure 2(c)).

Given that stitch type of embroidery and textile background can significantly impact the accuracy of a pattern's geometry,[29] two embroidery stitch types, Satin (S) and Tatami (T) (Figure 3), were selected for evaluation. Stitch directions were kept constant to ensure comparability. The woven and knitted fabrics were chosen as background to represent different weave types and material properties. The characteristics of the selected textiles are summarised in Table 2.

To ensure reliable results, Finder Pattern samples were prepared using a standardised machine embroidery procedure. Embroidery was carried out on a Ricoma MT-01 machine using Wilcom software and DBXK5-NY 80/12 needles. Madeira Classic No.40, Dtex135x2 threads were used along with a non-woven PES interlining (55 g/m^2) for support. The fabric swatch size was selected to fit the embroidery hoop and to ensure proper alignment throughout the stitching process. A schematic of the sample preparation process is presented in Figure 4.

Methodology

The embroidered samples were scanned at 300 dpi and saved in .tif format. The resulting images were processed using ImageJ software. The images were calibrated and converted to a binary format to remove visual noise such

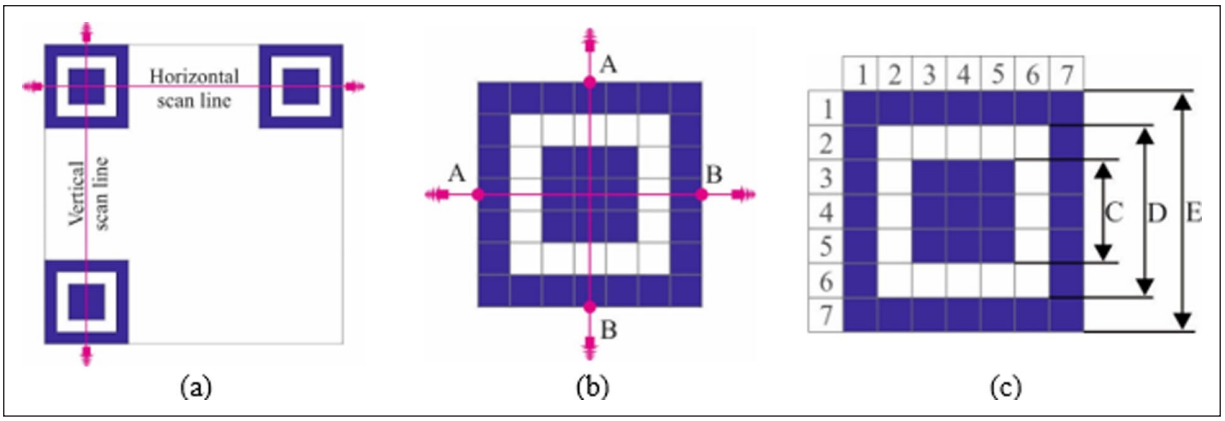

Figure 2. Finder pattern: (a) scan line directions, (b) scan line AB on element and (c) structure.

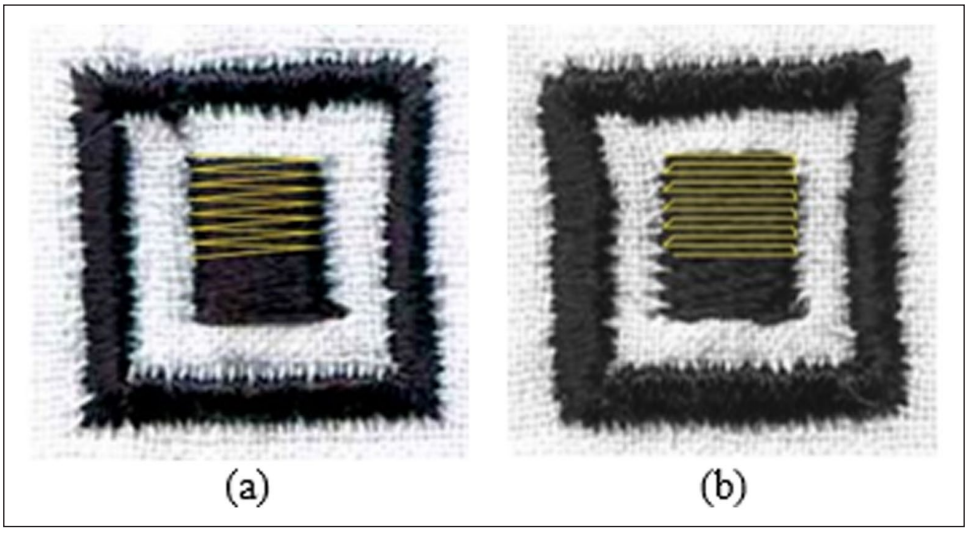

Figure 3. Machine embroidery stitch types: (a) satin stitch and (b) tatami stitch.

as background texture pixels. Inkscape software was used for measurements along vertical and horizontal scan lines (Figure 5(a) and (b)). The scan line was positioned manually, while the software function automatically detected and measured all elements intersecting the defined scan lines. It is essential to take measurements in both directions, as Finder Patterns appear in three corners of the QR code, and scanning devices evaluate both directions during recognition. Along scan line AB, modules covered by threads (black) are denoted by X_{bi}, while modules not covered by threads (white) are labelled by X_{wi}. Five segments were measured: X_{b1}, X_{w2}, $X_{b3\text{-}5}$, X_{w6}, and X_{b7} (Figure 5(c)). The central section, consisting of three black modules, was embroidered as a single unit and treated as one measurement, indexed $i = 3$–5. Consequently, the total theoretical length of scan line AB in the Finder Pattern was calculated using the following equation:

$$AB_T = 5X_b + 2X_w, \tag{1}$$

where AB - length of the scan line (mm), X_b - length of the black module (mm), X_w - length of the white module (mm).

The deviation (ΔX_i, %) was calculated by comparing the measured values (X_i) with the theoretical module (X_T) length as follows:

$$\Delta X_i = \frac{X_i - X_T}{X_T} \times 100, \tag{2}$$

where ΔX_i - deviation of the module i size (%), X_i - measured module i (mm), X_T - theoretical module size (mm).

The total deviation along scan line AB depends not only on the individual module deviation but also on their interaction. Therefore, the overall deviation (ΔAB, %) is expressed as:

$$\Delta AB = \frac{5\Delta X_b + 2\Delta X_w}{7}, \tag{3}$$

Table 2. Textile background properties.

Background/parameters	Woven	Knitted
Fabric weave	Plain weave (W)	Interlock Jersey (J)
Composition	100% cotton	100% PES
Area density, g/m^2	105	175
Thickness, mm	0.27	0.43
Density, threads/cm	warp – 29; weft – 27	N/A
Density, loops/cm	N/A	wale-16; course – 17

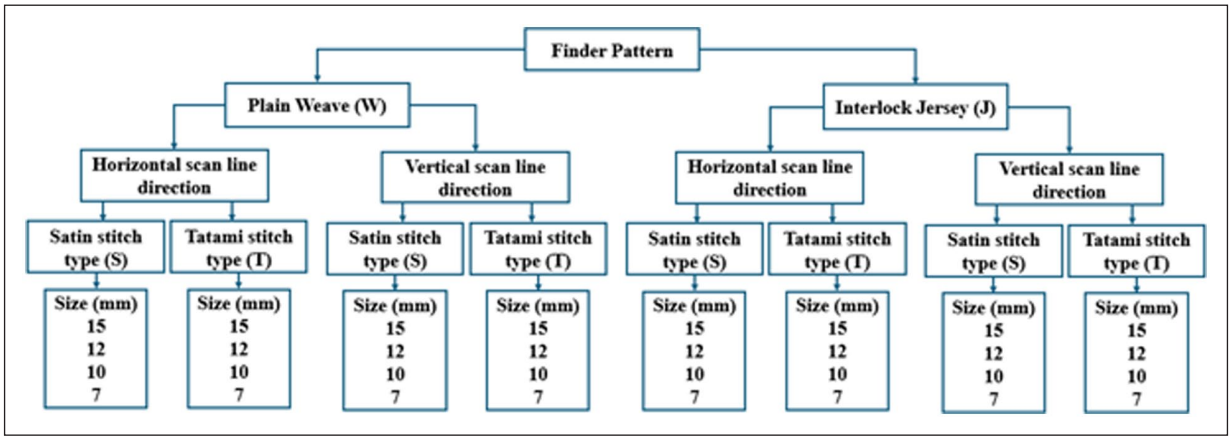

Figure 4. Sample preparation scheme.

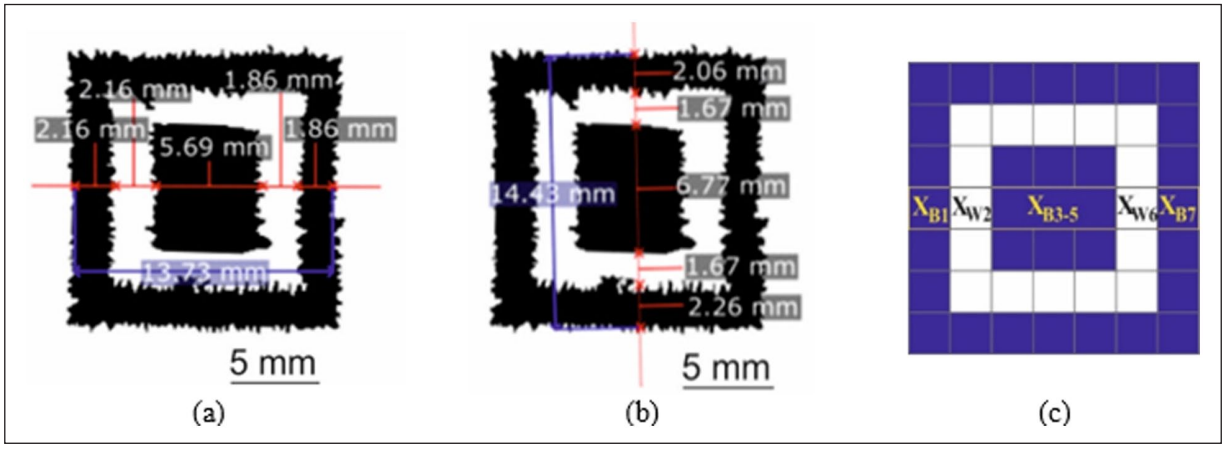

Figure 5. Finder Pattern: (a) horizontal axis measurements for sample W1-S-15, (b) vertical axis measurements for sample W1-S-15 and (c) modules indexing.

where ΔAB - deviation in can line (%), ΔX_b - deviation of modules covered by threads (%), ΔX_w - deviation of module not covered by threads size (%).

Statistical one-way ANOVA analysis was conducted using R Project software to determine the effect of each independent variable (fabric type, Finder Pattern size, scan line direction, stitch type) on the scan line AB length separately. The significance of each variable was assessed using *F*- and *p*-values across 32 experimental conditions (Figure 4), each repeated four times. Further on, a targeted two-way ANOVA was performed to examine the combined effect of fabric type and scan line direction, as this interaction was considered particularly relevant to the scanning process. Higher-order interactions were not included in this study to focus on the individual variable contribution and maintain clarity in results interpretation.

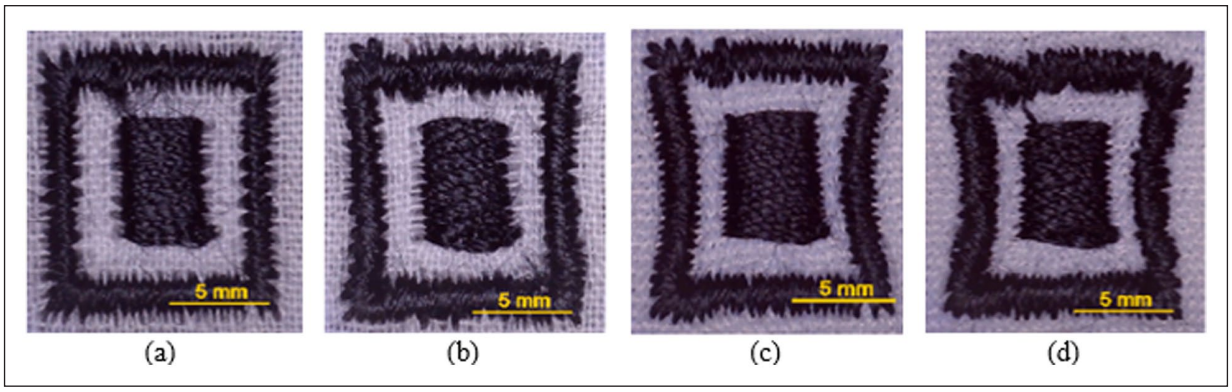

Figure 6. Samples of embroidered Finder Pattern elements: (a) W1-S-12 mm, (b) W1-T-12 mm, (c) J5-S-12 mm, (d) J5-T-12 mm.

Results and discussion

Deformations of embroidered finder pattern shape

An embroidery design was created to maintain the positioning of the Finder Pattern element as accurately as possible. However, geometric distortions were frequently observed at the edges of the element, particularly in the modules not covered by threads X_{w2}, X_{w6} (Figure 6), due to the processing of stitches by the embroidery machine. Fabric deformation during embroidery involves complex interplay between the fabric and the stitching threads, which induce localised stresses and strains that alter the fabrics weave. These distortions occur due to the interaction between the structure of the fabric (thread arrangement and density), embroidery stitch density and arrangement, together with the mechanical stresses induced by the embroidery process. Visual analysis of the embroidered samples revealed that the fabric type had a distinct influence on the geometric deviations along the horizontal and vertical scan lines. This effect was particularly pronounced in the knitted fabric (Figure 6(c) and (d)). In addition, a clear size-dependent effect was observed: the smallest Finder Pattern exhibited significantly greater module displacement than the larger ones, regardless of the fabric type (Figure 7).

These findings were confirmed by ANOVA test (Table 3) and showed that all four variables significantly affected scan line AB length. Although all factors were statistically significant ($p < 0.001$), the large difference in F-values highlights Finder Pattern size as the dominant contributor to scan line variability.

Size-dependent variation of Finder Pattern deviations

ANOVA analysis showed that the Finder Pattern size had the strongest and statistically highly significant effect on the scan line AB length (Table 3). As the size of module X is directly dependent on AB size (Table 1), modules covered by threads X_{b1} and X_{b5} exhibit the same tendency (Figure 8(a)). Analysis of the X module revealed distinct patterns based on different sizes. The variation is considerable, ranging from 3% to 45%. Modules $X_{b3\text{-}5}$ embroidered as a single unit and three times larger than individual modules showed lower deviations (ranging from –8% to +4%) and closely aligned with the theoretical values. Notably, the $X_{b3\text{-}5}$ module at the 7 mm Finder Pattern size exhibited a unique negative deviation, not observed in other modules covered by thread.

In general, with a few exceptions, all the modules covered by threads were larger than the theoretical size ($X_{bi} > X_T$). This increase is attributed to fabric displacement caused by needle penetration and the added volume of the thread within the fabric structure, which contributes to larger element dimensions. In contrast, the modules not covered by threads X_{w2} and X_{w4}, consistently exhibited negative deviations ($X_{wi} < X_T$) ranging between 19% and 40%.

The overall geometric deviation in the modules covered by threads ΔX_b showed a clear dependence on the size of the embroidered elements, whereas the deviation in the modules not covered by threads ΔX_w showed no such relationship. Because these two module types contribute differently to the overall deviation ΔAB (equation (3)), the total size of embroidered Finder Pattern along the scan line AB remains close to the theoretical values, with variations approximately from +3% to – 6% (Figure 8(b)).

Since ΔX_b had the greatest impact on the size of embroidered element, it was chosen as the primary parameter for further analysis. Although ΔX_w had a lower impact, both parameters contribute to the final geometric accuracy of the embroidered Finder Pattern. The estimated dependencies for ΔX_b, ΔX_w, and ΔAB as a function of scan line AB length are shown in Figure 9, providing a basis for selecting the most appropriate QR size for embroidery. The dependence describing ΔAB changes indicates that the most accurate result occurs when AB is 8,82 mm ($\Delta AB \approx 0\%$). This indicates that, under the research parameters, the optimal size of the embroidered QR code for version 2 is approximately

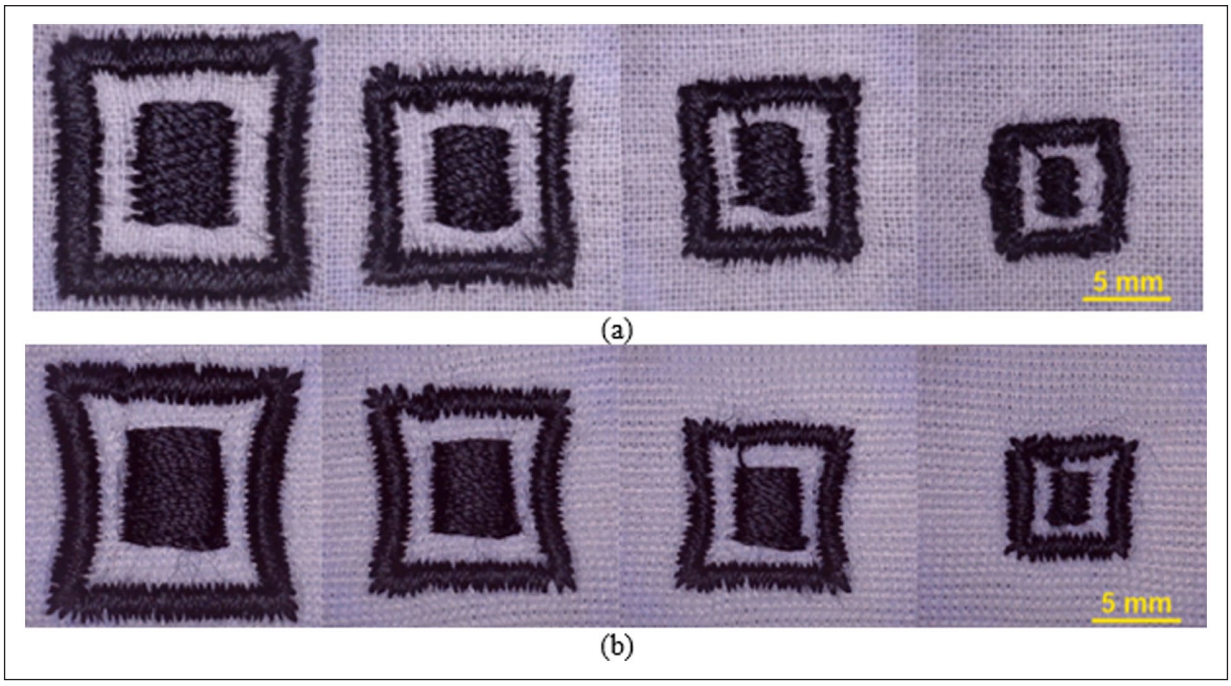

Figure 7. Samples of embroidered Finder Pattern elements: (a) W1-T when size changes from 15 mm till 7 mm, (b) J5-S when size changes from 15 mm till 7 mm.

Table 3. Effect of variables on scan line AB values.

No.	Variables	*F*-value	*p*-value	Significance
1	Finder Pattern size	13,223.394	$<2.2 \times 10^{-16}$	Highly significant
2	Scan line direction	233.583	$<2.2 \times 10^{-16}$	Significant
3	Fabric type	115.847	$<2.2 \times 10^{-16}$	Significant
4	Stitch type	73.204	6.20×10^{-14}	Significant

32 mm. The ΔX_w value for modules with no threads is nearly independent of element size, with an average deviation of −27.6% and a rate of change of approximately – 0.1% per 1 mm. Because the X_w modules do not receive stitch coverage, geometric deviations are concentrated mainly at the intersections with modules covered by threads. The final deviation ΔAB is primarily influenced by ΔX_b in embroidered zones, changing by around −1.5% per 1 mm.

Fabric-dependent variation in Finder pattern deviations

When evaluating deviations based on the textile background, the overall trends appear analogous to those previously described in relation to element size. Modules covered with threads X_b1 and X_{b7} were larger than the theoretical size X_T, with deviations ranging between 16% and 23%. The modules not covered by threads, X_{w2} and X_{w6}, were smaller than the X_T. In contrast, $X_{b3\text{-}5}$ were close to the theoretical size of 3_{XT}, with deviations within ± 1.5% (Figure 10(a)).

An analysis of fabric type influence showed that ΔX_b values for modules covered by threads are approximately 1.7 times lower for knitted fabric than woven fabric (Figure 10(b)). In contrast, ΔX_w for modules not covered by threads was approximately 1.5 times lower for woven than knitted fabric. Although the Finder Pattern contains more modules covered by threads (five of seven), the deviations of modules not covered by threads were large enough to cause a higher overall AB variation in the knitted fabric compared to the woven. These findings, combined with the results of the ANOVA analysis (Table 3), demonstrate that deviation is influenced by fabric structure and thread displacement.

As noted in Section 4.1, visual and ANOVA analyses showed that the geometry of the embroidered Finder Pattern is preserved differently along the vertical and horizontal axes. To reliably evaluate effects on AB length, both the textile background and scan line direction must be considered together. A focussed two-way ANOVA confirmed that the combined effect of fabric type and scan line direction was statistically significant ($F = 24.001$, $p = 3.21 \times 10^{-6}$). The results indicate that the influence of

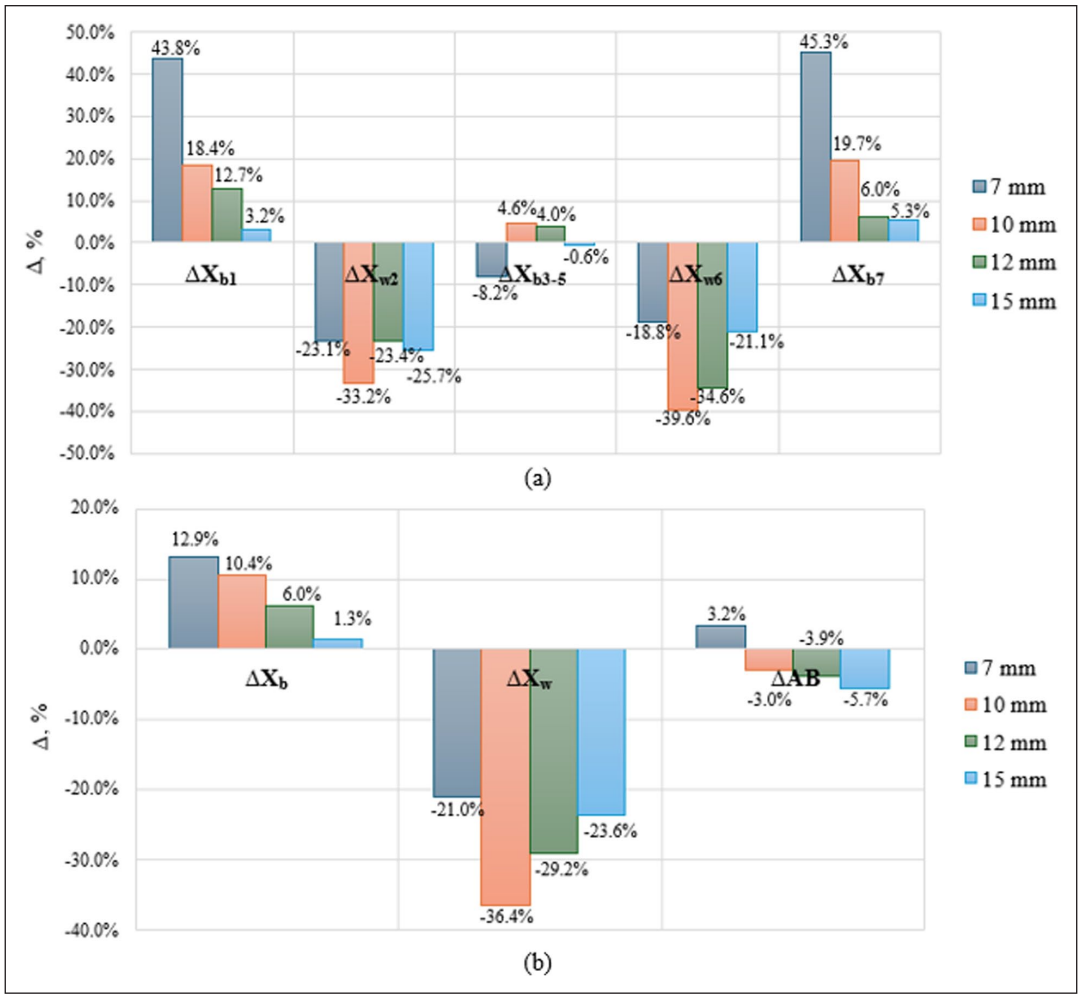

Figure 8. Deviation by Finder Pattern size: (a) individual module deviation, (b) module groups deviation.

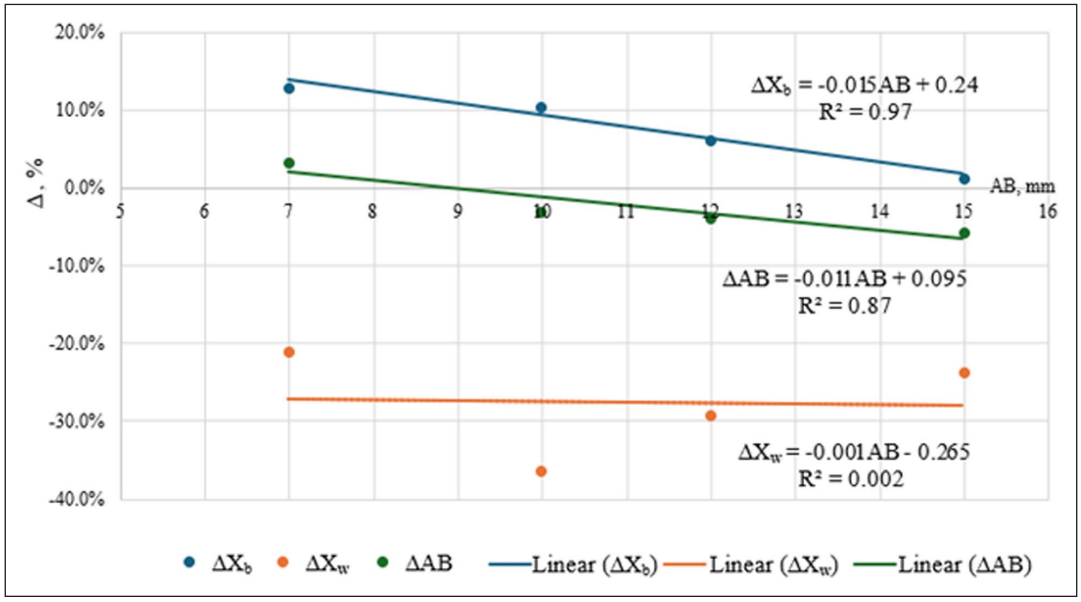

Figure 9. Deviations dependent on Finder Pattern size.

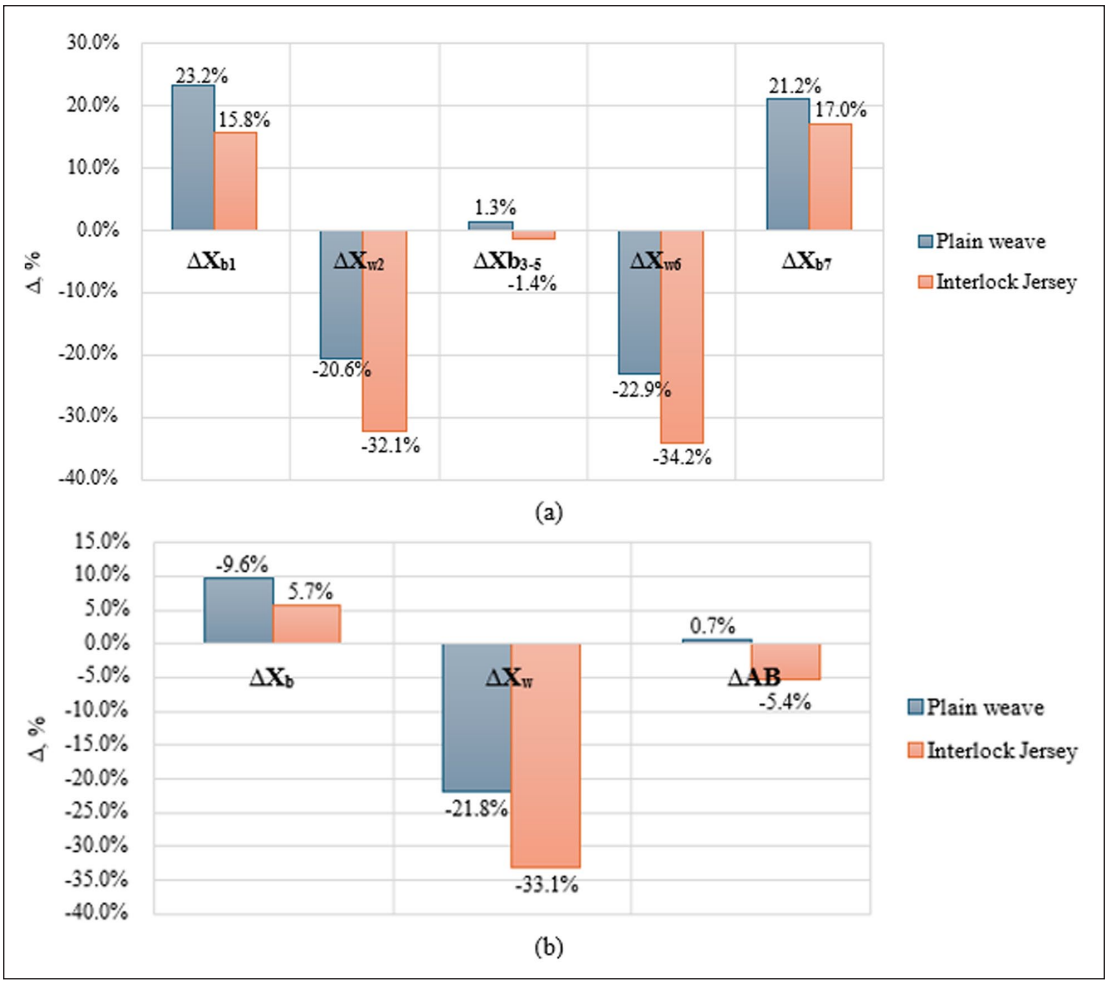

Figure 10. Deviation trends according to fabric type: (a) individual module deviation and (b) module groups deviation.

scan direction on AB length is fabric dependent and governed by the structural characteristics of each fabric type.

Individual module deviations (Figure 11(a)) showed no clear differences based on fabric type or scan line direction. However, the analysis of grouped modules and as well as AB deviation revealed pronounced differences (Figure 11(b)). The deviation of all modules covered with threads X_b on the horizontal axis was within 1%–3% of the theoretical size. In contrast, on the vertical axis, deviations were 5–10 times greater, between 11% and 16%. This trend was consistent across both fabric types. The deviations of modules not covered by threads X_w were largely similar, except for one outlier group on woven fabric in the horizontal direction, which showed approximately three times smaller deviation. However, when evaluating the overall geometric accuracy along AB, the largest deviation from the theoretical size was observed on the knitted fabric in the horizontal direction (−8.8%), indicating an increased risk for successful QR code readability. A notable case is the Finder Pattern geometry on the woven fabric along the vertical axis, the only group with positive ΔAB, while other groups remained negative, yet close to theoretical value. These results highlight the influence of fabric structure and anisotropic properties of the fabric on the quality of small elements, such as QR code Finder Pattern and they align with the visual and statistical analysis of the embroidered samples (Figure 6).

Influence of embroidery stitch type on the Finder Pattern deviations

Although stitch type had the least effect on AB length among the four variables (Table 3), it was still statistically significant and influenced the Finder Pattern dimensions. An analysis shows that individual X_b modules filled using satin stitches are approximately twice as accurate as those filled with tatami stitches (Figure 12(a)). However, when evaluating the grouped 3X modules placed adjacently, the fill type had almost no effect because these modules are embroidered as a single unified element. Modules not covered by threads (X_{w2} and X_{w6}) were not directly influenced by the stitch type and their deviations reflected the same patterns observed for element size and fabric type.

Analysis of grouped module data (Figure 12(b)) showed that ΔX_b values indicate that satin fill is nearly three times

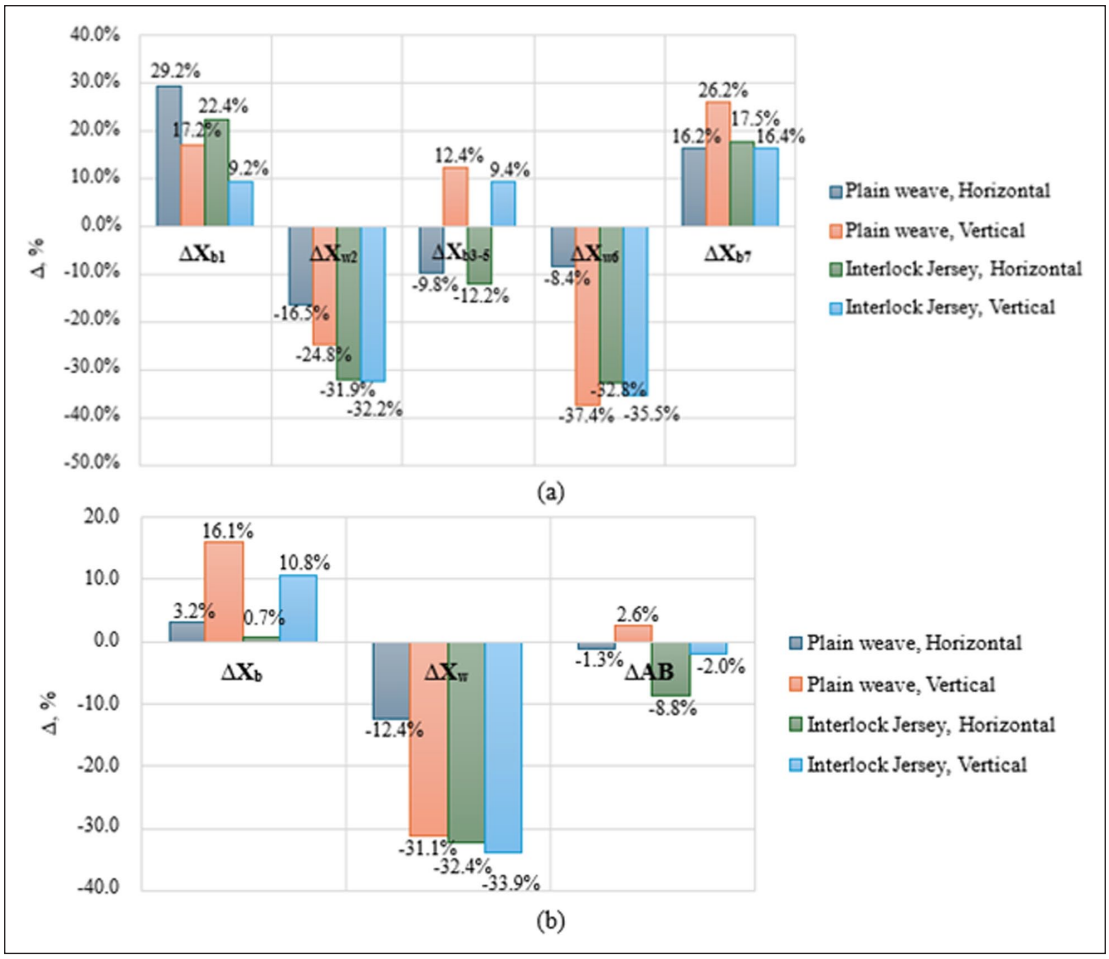

Figure 11. Geometric deviations depending on scanning axis and fabric type: (a) individual module deviation and (b) module groups deviation.

more accurate than tatami. Although the non-embroidered zones are not directly related to the stitch type, they still affect the overall ΔAB. As ΔX_w values remained relatively high (25% and 29%), the overall AB geometry was more accurate in the case of tatami embroidery. Considering that a QR code also includes other patterns often composed of single modules, satin stitch is recommended as the preferred stitch type for embroidery.

Conclusions

This study is the first to investigate the accuracy of QR codes embroidered on textiles using Pattern Finder analysis, as specified in ISO/IEC 18004. Assessing the quality of embroidered QR codes using the total length of scan line AB defined in the standard is challenging and requires a detailed examination of structural elements, including individual modules. These findings clearly demonstrate the need for a detailed analysis of the quality of embroidered QR codes and the development of specific recommendations for their production and quality assessments.

The accuracy of the embroidered QR code geometry depends on multiple variables, including the code size, fabric type, embroidery stitch type, and scan line direction. The study revealed that modules covered by threads tended to exceed their theoretical dimensions (deviations ranging from +3% to 45%), while modules not covered by threads were generally smaller and showed no consistent correlation with these variables (deviations ranged from −40% to −11%). Central modules were the most dimensionally stable with deviations from −6% to +3%.

Finder Pattern size significantly affected the precision of the scan line AB length, demonstrating that changes in element size systematically alter how individual module deviations propagate to the overall pattern. For the woven fabric and vertical scan line direction for knitted fabrics, the AB deviations remained within –2% to +2.6%, whereas the horizontal scan line direction for knitted fabrics showed up to four-time higher distortions (–8.8%). This shows that embroidery influences distortions of QR codes on knitted fabrics and increases the risk of unreadability under real-use conditions. Tatami stitch produced a more accurate overall shape of the Finder Pattern (ΔAB=–0.4%) compared to

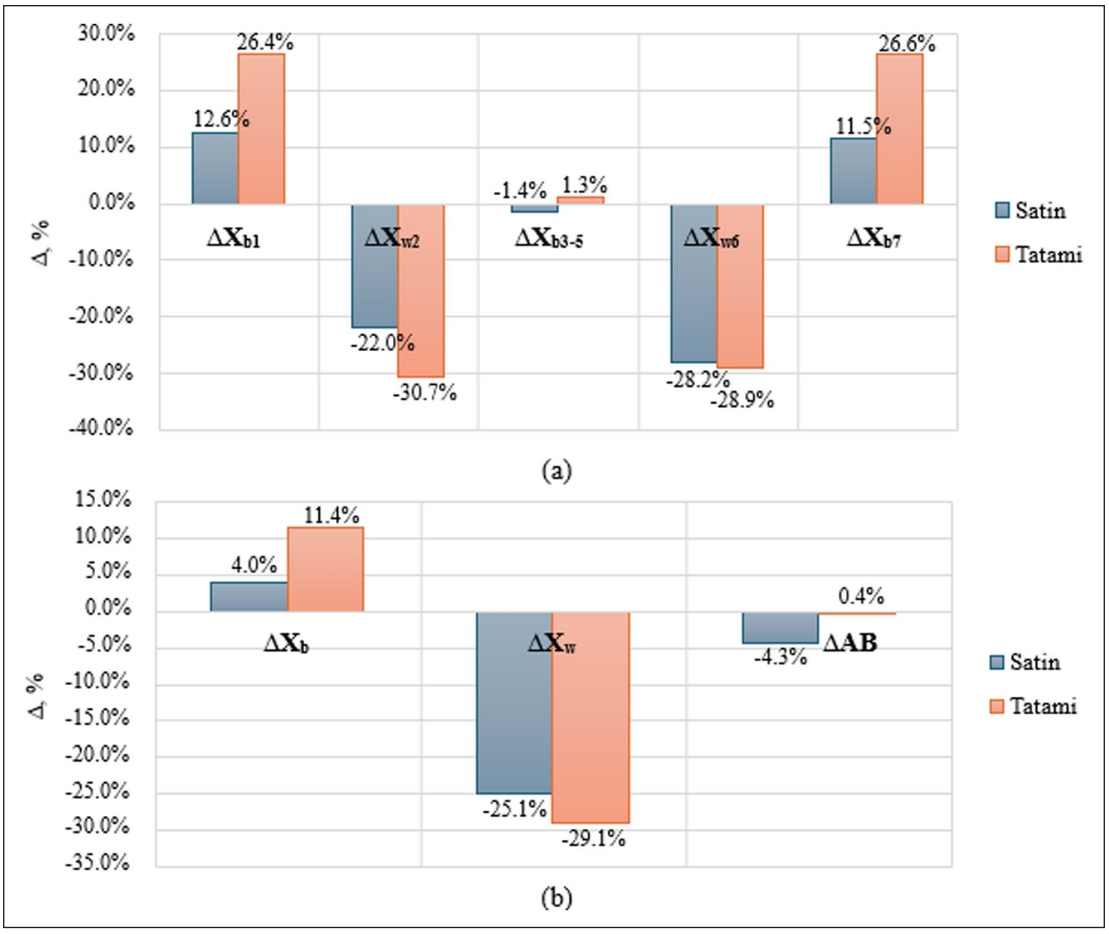

Figure 12. Accuracy of (a) individual and (b) grouped Modules by embroidery stitch type.

satin stitch (ΔAB = –4.3%), although satin stitch resulted in more precise individual modules (average deviation for satin –4.3% and +11.5% for tatami).

These findings confirm that embroidery technologies can successfully embed functional QR codes in textiles. ANOVA analysis proved that the most significant variable for AB length is Finder Pattern size, with F value of 13,223, while other variables had F values ranging from 73 to 234 ($p < 0.001$). However, embroidery parameters must be carefully aligned with variables such as embroidery stitch type and fabric characteristics. To achieve optimal quality, the Finder Pattern module size should be approximately 8.82 mm, corresponding to a total QR code dimension of about 32 mm for QR code version 2. Woven fabrics are generally more suitable as a background, while knitted fabrics require more precise parameter control. Considering the complex geometry of QR codes, satin stitch is recommended for its superior precision in shaping individual modules.

Future research should focus on the durability and practical performance of embroidered QR codes in textile applications. The effects of accelerated ageing, repeated laundering and mechanical stress on module geometry should be evaluated to ensure long-term readability. Moreover, this study may provide valuable insights for other smart tag integrations using embroidery, such as NFC or RFID systems, where high geometric precision, repeatability, and durability are equally critical.

Acknowledgements

The authors would like to thank PhD. Jovita Dargiene for her expert guidance on embroidery techniques and advice for the preparation of experimental samples, and also gratefully acknowledge PhD. Vaida Bartkute-Norkuniene for valuable assistance during statistical analysis.

ORCID iDs

Breitmozere Inga https://orcid.org/0009-0005-2104-965X
Domskiene Jurgita https://orcid.org/0000-0001-7276-522X

Funding

The authors received no financial support for the research, authorship, and/or publication of this article.

Declaration of conflicting interests

The authors declared no potential conflicts of interest with respect to the research, authorship, and/or publication of this article.

References

1. Ji Y and Jiang G. Garment customization big data–processing and analysis in optimization design. *J Eng Fibers Fabr* 2020; 15: 1–7.
2. Adisorn T, Tholen L and Götz T. Towards a digital product passport fit for contributing to a circular economy. *Energies* 2021; 14(8): 2289.
3. Jansen M, Meisen T, Plociennik C, et al. Stop guessing in the dark: identified requirements for digital product passport systems. *Systems* 2023; 11(3): 123.
4. King MRN, Timms PD and Mountney S. A proposed universal definition of a digital product passport ecosystem (DPPE): worldviews, discrete capabilities, stakeholder requirements and concerns. *J Clean Prod* 2023; 384: 135538.
5. Siliņa L, Dāboliņa I and Lapkovska E. Sustainable textile industry – wishful thinking or the new norm: A review. *J Eng Fibers Fabr* 2024; 19: 1–27.
6. Gligoric N, Krco S, Hakola L, et al. SmartTags: IoT product passport for circular economy based on printed sensors and unique item-level identifiers. *Sensors* 2019; 19(3): 586.
7. Vazquez-Briseno M, Hirata FI, Sanchez-Lopez J, et al. Using RFID/NFC and QR-code in mobile phones to link the physical and the digital world. In: Deliyannis I (ed.) *Interactive Multimedia, InTech*; 2012: pp.219–242.
8. Tarjan L, Šenk I, Tegeltija S, et al. A readability analysis for QR code application in a traceability system. *Comput Electron Agric* 2014; 109: 1–11.
9. Han J, Wang G and Sidén J. Fragment-type UHF RFID tag embedded in QR barcode label. *Electron Lett* 2015; 51(4): 313–315.
10. Isohanni J. Use of functional ink in a smart tag for fast-moving consumer goods industry. *J Packag Technol Res* 2022; 6(3): 187–198.
11. Galiyawala HJ and Pandya KH. To increase data capacity of QR code using multiplexing with color coding: An example of embedding speech signal in QR code. In: *2014 Annu IEEE India Conf (INDICON)*, Pune, India, December 11–13, 2014, pp.1–6.
12. Legardeur J and Ospital P. *Digital product passport for the textile sector*. Study, European Parliamentary Research Service, PE 757.808, June 2024.
13. Fan J, Bao B, Wang Z, et al. Flexible, switchable and wearable image storage device based on light responsive textiles. *Chem Eng J* 2021; 404: 126488.
14. Li P, Sun Z, Wang R, et al. Flexible thermochromic fabrics enabling dynamic colored display. *Front Optoelectron* 2022; 15(1): 40.
15. Nofal RM. Initiating android phone technology using QR codes to make innovative functional clothes. *Int J Clothing Sci Technol* 2020; 32(6): 935–951.
16. Vorobchuk M, Pashkevych K, Yezhova O, et al. QR code design: From digital graphics to environmental, product and fashion design. *J Graph Eng Des* 2024; 15(2): 51–57.
17. Kuusk K, Wensveen SAG and Tomico O. Crafting qualities in designing QR-coded embroidery and bedtime stories. In: *The 5th Conf on the Art of Research*. Aalto University, Helsinki, Finland, November 2014, pp.1–12.
18. Mustafa B, Mohamed SS and Hafez NM. The aesthetical impacts of quick response (QR) codes in apparel design to revitalize handcrafts. *Int Des J* 2025; 15(1): 150–170.
19. Daukantienė V and Laurinavićiūtė I. The synergism of design and technology for the optimisation of embroidery motifs in clothing. *Int J Clothing Sci Technol* 2013; 25(5): 350–360.
20. Zhenyuan L, Piovarči M, Hafner C, et al. Directionality-aware design of embroidery patterns. *Comput Graph Forum* 2023; 42(2): 397–409.
21. Daukantienė V and Mikelionytė K. Investigation of the influence of technology parameters and thread type on embroidered textile element quality. *Autex Res J* 2020; 20(4): 517–523.
22. Bahadir Ünal Z and Acar E. Investigation of the effect of using different interlinings on the comfort properties of the embroidered surface. *Textile Leather Rev* 2022; 5: 165–179.
23. Boz S. Investigation of the effects of embroidery parameters on physical properties and thermal comfort. *Tekstil Konfeksiyon* 2022; 32(1): 86–92.
24. Bulathsinghala RL. Investigation on material variants and fabrication methods for microstrip textile antennas: A review based on conventional and novel concepts of weaving, knitting and embroidery. *Cogent Eng* 2022; 9(1): 2025681.
25. Rafiq M, Imran A, Rasheed A, et al. A review on the manufacturing techniques for textile based antennas. *J Eng Fibers Fabr* 2024; 19(3): 1–18.
26. Seager R, Zhang S, Chauraya A, et al. Effect of the fabrication parameters on the performance of embroidered antennas. *IET Microw Antennas Propag* 2013; 7(14): 1174–1181.
27. Kuo CFJ and Juang Y. A study on the recognition and classification of embroidered textile defects in manufacturing. *Text Res J* 2016; 86(4): 393–408.
28. Radavičienė S, Jucienė M, Juchnevičienė Ž, et al. Analysis of shape nonconformity between embroidered element and its digital image. *Mater Sci* 2014; 20(1): 84–89.
29. Juchnevičienė Ž, Jucienė M, Dobilaitė V, et al. The research on the accuracy of the geometrical parameters of the closed-circuit embroidery element. *Mater Sci* 2018; 24(4): 453–459.
30. Zheng Y, Jin L, Qi J, et al. Performance evaluation of conductive tracks in fabricating e-textiles by lock-stitch embroidery. *J Ind Text* 2022; 51(4_suppl): 6864S–6883S.
31. ISO/IEC 18004. 2024. Information technology — Automatic identification and data capture techniques — QR code bar code symbology specification
32. TQRCG: QR Code generator, https://www.the-qrcode-generator.com/ (accessed 19 January 2024).
33. Kulkarni SS and Malagi C. Creation and analysis of QR code. *Bonfring Int J Softw Eng Soft Comput* 2016; 6: 86–89.
34. Shokeen G, Aggarwal S and Bhatia MK. QR code analysis. *Int J Res Appl Sci Eng Technol* 2022; 10(12): 747–752.
35. Karrach L, Pivarčiová E and Božek P. Identification of QR code perspective distortion based on edge directions and edge projections analysis. *J Imaging* 2020; 6(7): 67.
36. Teoh MK, Teo KTK and Yoong HP. Numerical computation-based position estimation for QR code object marker: mathematical model and simulation. *Computation* 2022; 10(9): 147.
37. Pavlović Ž, Dedijer S, Pál M, et al. Readability of screen printed QR codes depending on their dimension, encoded content and type of printing substrate using screen printing technique. *J Chem Technol Environ* 2018; 7(12): 37–45.